THE JOURNAL OF PHYSICAL CHEMISTRY C

Article

pubs.acs.org/JPCC

Modeling $LiNbO_3$ Surfaces at Ambient Conditions

Rebecca Hölscher, Wolf Gero Schmidt, and Simone Sanna*

Lehrstuhl für Theoretische Physik, Universität Paderborn, 33095 Paderborn, Germany

ABSTRACT: The adsorption of N_2, O_2, CO_2, CH_2, H_2, N_2O, CO, and H_2O on $LiNbO_3$ (0001) surfaces is simulated from first-principles in order to better understand its properties under ambient conditions. The adsorption energies and geometries, as well as the chemical bonding characteristics, are determined. Striking differences in the adsorption behavior at oppositely polarized surfaces are found. The effect of the adsorbed molecules on the surface charge is investigated. Phase diagrams for the adsorption of the different species dependent on pressure, temperature, and environment humidity are presented. They indicate that the desorption temperatures depend not only on the molecular species but also on the polarity of the surface.

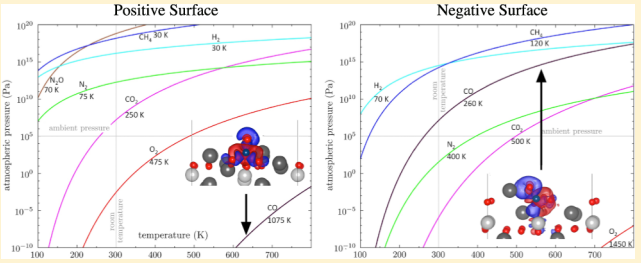

INTRODUCTION

Lithium niobate [$LiNbO_3$ (LN)] is one of the most versatile materials for (nonlinear) optics and acoustic applications. Surface acoustic wave devices,[1] second harmonic generation, and frequency modulators[2] are examples of applications which exploit its unusual and valuable properties, such as the strong photorefractivity or the pyro- and piezoelectricity.[2] While traditional applications are mainly based on the relatively well understood bulk properties, the (0001) surfaces and their chemical properties recently came into the focus of both research and applications. One intriguing perspective is the possibility of using lithium niobate as a chemical sensor by detecting the adsorption-induced polarization modifications.[3] However, the understanding of the (0001) surfaces at the atomic level is just at its beginning and is restricted to the limiting cases of surfaces in vacuum or in aqueous solution. Little is known about the surface under ambient conditions. This is mainly because the surface is experimentally very challenging: In the ferroelectric phase[4] (stable below 1486 K) the z surfaces are highly polar.[5] Charging effects prohibit the application of electron tunneling or diffraction techniques, and unscreened surface charges hinder atomic force microscopy under ambient conditions.[6] An ideal bulk cut perpendicular to the c-axis results in a surface charge density (SCD) of 0.7 C/m^2. However, different mechanisms compensate the surface charge. Johan and Soergel have determined the SCD of the z surfaces of undoped congruent LN at ambient conditions by piezoresponse force microscopy,[7] measuring a value of 140 $\mu C/m^2$. This value proves the efficiency of the charge compensation. As pointed out in ref 8, several charge compensation mechanisms may contribute to stabilize polar surfaces. Aside from internal mechanisms such as ionic and electronic charge redistribution, external mechanisms such as molecular adsorption may reduce the polarization charge. Indeed, different charge compensation mechanisms occur at the LN z surfaces at different temperature regimes: LN surfaces are nonstoichiometric,[9−12] show reconstruction patterns at temperatures above 1100 K, and adsorb foreign atoms and molecules to reduce the large polarization charge at lower temperatures.[13] Water molecules are known to efficiently screen surface charges.[14,15] The contribution of internal surface phenomena to the charge compensation was recently investigated theoretically for surfaces in vacuum.[6] However, nothing is known about surfaces at ambient conditions. In the following we will investigate the effect of external stabilization mechanisms, that is, the adsorption of foreign adsorbates; thereby adsorption site and geometry of the most common air components N_2, O_2, CO_2, CH_4, H_2, N_2O CO and H_2O are determined. Adsorption phase diagrams are then extracted from these data and reveal the desorption temperature of the different adsorbates depending on pressure and temperature. The influence of the adsorbed molecules on the surface morphology and charge density is discussed in detail. While the positive surface morphology is relatively unaffected by the adsorbates, the negative surface undergoes important structural modifications upon molecular adsorption. The results of this investigation can be used, among others, for the interpretation of temperature-programmed desorption experiments.

METHODOLOGY

Total energy calculations within the PW91 formulation of the generalized gradient approximation (GGA)[16] as implemented in VASP (Vienna ab initio simulation package)[17] are performed to simulate the adsorption of various adsorbates. Thereby we employ projector augmented wave (PAW)[18] potentials as in our previous works.[14] The electronic wave functions are expanded into plane waves up to a kinetic energy of 400 eV and a Γ centered 2 × 2 × 1 k-point mesh is used to carry out the

Received: March 25, 2014
Revised: April 29, 2014
Published: April 29, 2014

 © 2014 American Chemical Society dx.doi.org/10.1021/jp502936f | J. Phys. Chem. C 2014, 118, 10213−10220

integration over the Brilliouin zone. The slabs modeling the substrate consist of 18 atomic layers stacked along the z direction, corresponding to 6 trilayers of LN and the respective surface termination (see Figure 1). At the positive surface (also

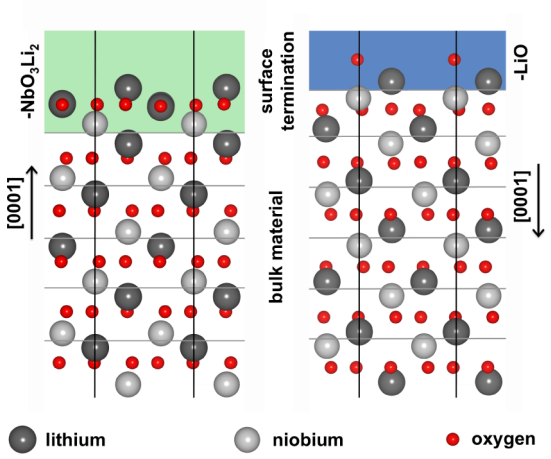

Figure 1. Slab used to model the thermodynamically stable LN(0001) surfaces. The positive surface termination is represented in green, while the negative is in blue. Horizontal lines separate the LN bulk-trilayers.

referred to as $+z$) the termination consists of an additional LN trilayer plus a lithium atom diffused into the oxygen layer. At the negative surface ($-z$) a layer of lithium and oxygen forms the surface termination.[9,10] The atoms in the five lowest layers of the material are kept frozen at their bulk positions to simulate the semi-infinite bulk material during the calculations. The remaining atoms including the adsorbates are free to relax without any constraints until the forces acting on every atom are lower than 50 meV/Å. Owing to the periodic boundary conditions the adsorbates and the slab interact with their periodic images. A 2 × 2 repetition of the surface unit cell is used to minimize the artificial interaction between adsorbates in the lateral directions (x and y). The resulting slabs (128 atoms for the $+z$ surface and 124 atoms for the $-z$ surface) model the adsorption of isolated molecules. The adsorption of one molecule per four substrate unit cells corresponds to an intermolecular distance of 10.3 Å, and models approximate the zero-coverage limit. A vacuum layer of about 16 Å separates the slabs. Dipole corrections[19,20] are used to account for the interaction of the slab with its periodic images. The corrections allow for the definition of a vacuum level at each slab side and thus for the calculation of work functions. The molecular gas phase is simulated by a single molecule in a cube with an approximate 25 Å edge.

The desorption temperature of the investigated adsorbates is estimated by comparing the grand (Landau) potential of the molecules adsorbed and that in the gas phase. This is calculated following ref 14 as

$$\Omega(n) = \frac{1}{A}[F(n) - \sum_i n_i\mu_i] \approx \frac{1}{A}[E^{\mathrm{tot}}(n) - \sum_i n_i\mu_i] \tag{1}$$

The free energy F of the surface can be approximated by the total energy E^{tot} of the surface, assuming entropic contributions of clean and adsorbed surfaces to be of similar magnitude. Thereby μ_i represents the chemical potential, and n_i is the number of adsorbed molecules of molecular species i per unit cell. The present study does not consider coadsorption of different molecular species and is restricted to the zero-coverage limit. The value of the grand potential is normalized to the size of the surface unit cell A. The intersection of the grand potentials of the clean and the (single molecule) adsorbed surface marks the chemical potential at which the molecule ad- or desorbs at/from the surface. The corresponding $\Delta\mu_i$ values which characterize the desorption limit can be related to specific experimental conditions characterized by desorption temperatue T and desorption pressure p, following ref 21. For the chemical potential in the approximation of the ideal di- or polyatomic gas this leads to

$$p(T) = \frac{m_i(k_BT)^{5/2}}{(2\pi\hbar^2)^{3/2}} \exp\left(\frac{\Delta\mu_i}{k_BT}\right) Z_i^{\mathrm{rot}} Z_i^{\mathrm{vib}} \tag{2}$$

where k_B is the Boltzmann constant and Z_i^{rot} and Z_i^{vib} are the rotational and vibrational partition functions of the molecules. The determination of $\Delta\mu i$, is shown exemplarily for N_2 in the next section. The partition functions differ for di- and polyatomic molecules, while the rotational partition function is defined as

$$Z_i^{\mathrm{rot}} = \begin{cases} \dfrac{2k_BTI_i}{\hbar^2} & \text{diatomic} \\ \dfrac{2k_BTI_i}{\sigma_i\hbar^2} & \text{polyatomic and linear} \\ \dfrac{(2k_BT)^{3/2}(\pi I_i^1 I_i^2 I_i^3)^{1/2}}{\sigma_i\hbar^3} & \text{other polyatomic} \end{cases} \tag{3}$$

the vibrational partition function is defined as

$$Z_i^{\mathrm{vib}} = \begin{cases} \dfrac{1}{1 - \exp -\frac{\hbar\omega_i^{\alpha}}{k_BT}} & \text{diatomic} \\ \prod_{\alpha}\left(\dfrac{1}{1 - \exp -\frac{\hbar\omega_i^{\alpha}}{k_BT}}\right) & \text{polyatomic} \end{cases} \tag{4}$$

Here m_i is the mass and the I_i are the momenta of inertia of the molecules, which are scalar quantities for dimers and tensors with the three component I_i^j in the case of polyatomic molecules. σ_i accounts for the symmetry of the molecules. Experimental values from ref 22 have been used in this work for the vibrational frequencies and momenta of inertia. The described approach represents a generalization of the method first proposed in ref 23.

RESULTS

Adsorption Site. To investigate possible adsorption sites for the most important air components, the potential energy surfaces (PES) for the adsorption of single molecules on both z surfaces are calculated. Since the surface structure of the LN(0001) is very complex, it is not sufficient to simulate the adsorption on a few high symmetry points of the unit cell. Therefore, the adsorption on an equidistant mesh of 48 points at the surface unit cell is tested, resulting into the PES shown in Figure 2. This mesh has proven to be dense enough[14] to capture local and global potential minima. The PES are calculated by constraining the lateral positions of one

dx.doi.org/10.1021/jp502936f | J. Phys. Chem. C 2014, 118, 10213−10220

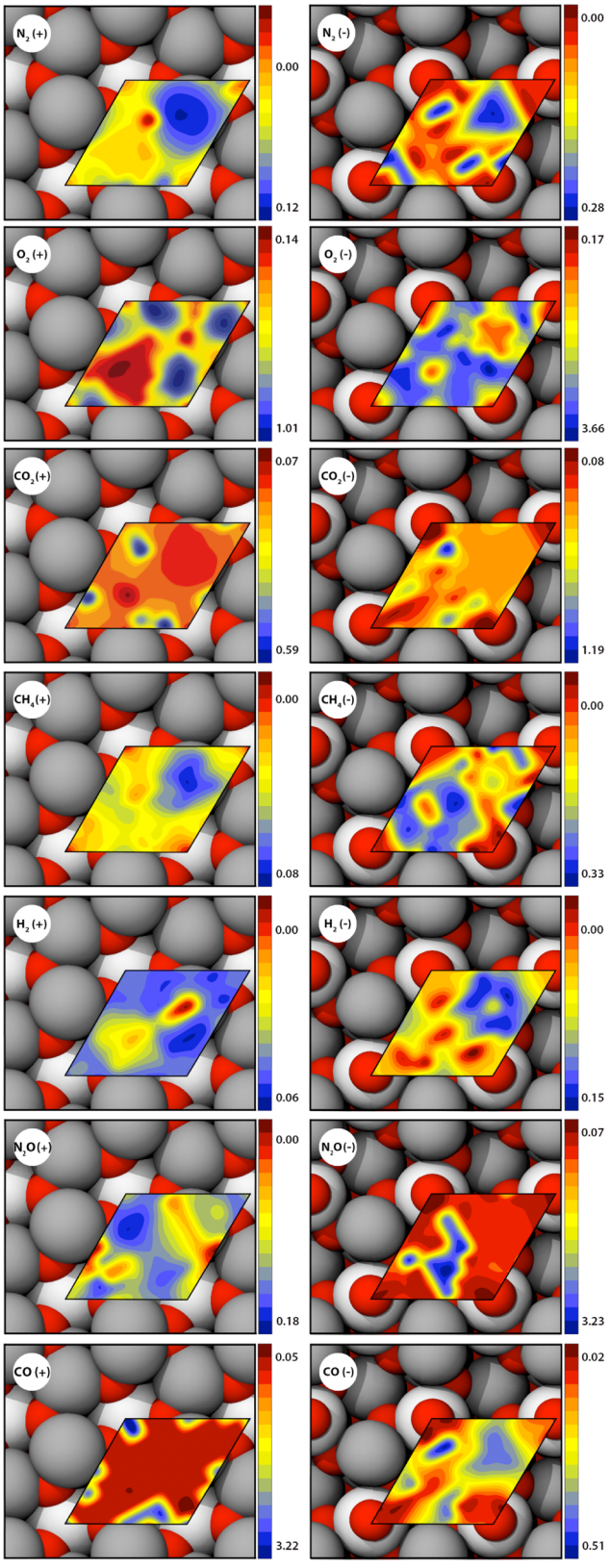

Figure 2. Potential energy surfaces for the adsorption of single molecules at the at the positive (left-hand side, labeled by +) and negative (right-hand side, labeled by −) $LiNbO_3(0001)$ surfaces. Energies in eV, atomic color coding as in Figure 1

(reference) atom and allowing the surface and other atoms of the surface to relax freely. Because of the presence of the lateral constraint limiting the degrees of freedom of the system, the PES energy is not the adsorption energy. It only yields qualitative information about favorable and unfavorable adsorption sites. Depending on the molecule shape and symmetry, a different number of starting configurations at each mesh point is used to find the global potential minimum.

The PES for the adsorption of N_2 at the positive surface (Figure 2) shows that molecular nitrogen favors the adsorption on top of the higher lithium atom of the surface termination. The slight energy differences between favorable and unfavorable regions as well as a broad and flat minimum in the PES suggest a high surface mobility of the molecule. On the negative surface, a much more corrugated energy landscape is observed. However, the global minimum for the molecular adsorption site is on top of the topmost lithium atom, as in the case of the positive surface. O_2 favors adsorption sites near oxygen atoms on both surfaces, however avoiding the topmost oxygen at the negative surface. At both surfaces the PES minima are more than 1 eV deep, suggesting a considerable surface affinity of the molecule. At the negative surface a delocalized energy minimum indicates a high surface mobility. The PES for the adsorption of CO_2 are characterized by strongly localized minima. These PES are calculated using the C atom as the reference atom. The minima are formed with the carbon atom almost on top of Nb and the oxygen atom oriented toward the Li atom at both surfaces. Relatively large energies (0.6 to 1.2 eV), suggest a large surface affinity for carbon dioxide. CH_4 seems to avoid the positions on top of the Nb atoms and adsorbs on top of the uppermost Li atom at the positive surface and close to the (not topmost) oxygen at the negative surface. H_2 shows a lower surface affinity, with PES minima as deep as 0.06 and 0.15 eV at the positive and at the negative surface, respectively. Furthermore, the minima are strongly delocalized, in particular at the positive surface. This results in a high surface mobility of the molecule. Interestingly, adsorption minima at the two LN(0001) sides are complementary: while at the $+z$ surface only positions near lithium atoms are avoided, the global minima at the $-z$ surface lie around the topmost Li. H_2 is the only molecule causing no distortion at all at the negative surface. The potential energy surface for the adsorption of the N_2O molecule is strongly polarization dependent. The positive face is characterized by a shallow (0.18 eV) and strongly delocalized minimum yielding high surface mobility. The PES at the negative surface is very corrugated instead, and the adsorption is only favored if the reference atom (the central nitrogen) is in a very localized area close to the lower Li surface atom. Carbon monoxide (CO) shows the deepest PES minima at the positive surface (3.2 eV) among the investigated adsorbates. The strongly localized minima indicate a low surface mobility of the molecule. On the negative surface the PES minima are five times smaller and localized in the neighborhood of the topmost Li atoms.

Adsorption Configuration. The adsorption geometry of the molecules is calculated starting with the molecules in one or more favorable adsorption sites individuated with the PES and relaxing all atomic degrees of freedom without any constraints. Sampling all the minima identified in the previous paragraph allows for the determination of the global adsorption minimum. Often, several final configurations of rather similar energy are possible. In the following only the energetically most stable configuration will be discussed. The adsorption energies are listed in Table 1, the adsorption configuration is represented in Figure 3, and the electronic charge redistribution upon

dx.doi.org/10.1021/jp502936f | J. Phys. Chem. C 2014, 118, 10213−10220

Table 1. Adsorption Energies of the Considered Molecules and Atoms, at the Positive (E^{p}_{ads}) and the Negative (E^{n}_{ads}) Surface, and Molecular Binding Energy in the Gas Phase E_b. All Values in eV, OH, and H_2O from previous works

adsorbate	E^{p}_{ads}	E^{n}_{ads}	E_b
N_2	0.12	0.75	16.33
O_2	1.04	3.76	8.52
CO_2	0.66	1.44	22.53
CH_4	0.08	0.31	17.83
H_2	0.06	0.16	6.68
N_2O	0.19	3.02	20.92
CO	3.84	0.80	14.50
OH[25]	2.94	5.71	6.98
H_2O[14]	0.61	1.28	14.01
H[25]	6.01	3.77	
C	9.35	6.06	
N	6.67	6.93	
O	4.56	7.57	

molecular adsorption is shown in Figure 4. The latter is calculated subtracting the electronic charge density of the isolated surface and molecule from those of the adsorbed system. The adsorption configuration and charge distribution of water molecules have been discussed in a previous work[14] and will not be repeated here.

The N_2 molecule adsorbs at the positive LN(0001) perpendicular to the surface at a distance of 2.26 Å from the topmost lithium atom (Figure 3). Thereby the relatively low adsorption energy of 0.12 eV and the charge distribution suggest a physisorbed molecule. If the N_2 molecule is tilted from the vertical line, the adsorption energy nearly drops to zero. At the negative surface the adsorption energy increases to a value of 0.75 eV. Again, the adsorption on top of the Li atom is favored. Close to the adsorption site, Li atoms are lifted by 1.32 Å from their original position to form bridge-like structures consisting of Nb−O−Li−O-Nb constructions. These structures are a common feature at the negative surface and occur upon adsorption of different molecules.

O_2 adsorbs at the $+z$ cut surface on top of an oxygen atom with an energy of 1.05 eV. Thereby the adsorbed molecule closely resembles an ozone like configuration. Ozone,[22] has a bond length of 1.28 Å and a bond angle of 116.8° while the structure at the LN(0001) surface has larger bond lengths of 1.45 and 1.31 Å and an angle of about 111.1°. On the $-z$ cut surface O_2 adsorbs flat on the surface (Figure 3). Bridge structures as occurring in the case of the N_2 adsorption are formed. The adsorption energy of 3.76 eV is the highest calculated adsorption energy on this surface. The charge distribution of Figure 4 shows a sizable charge accumulation between molecule and substrate, and suggests a chemisorbed molecule forming a covalent bond with the oxygen surface atoms for both polarization directions.

CO_2 adsorbs with a rather distorted structure on both surfaces (see Figure 3), which are reminiscent of a CO_3 molecule. CO_3 has calculated C−O bond lengths between 1.24 and 1.27 Å in the D_{3h} symmetry.[24] On the positive surface we find the C−O bond perpendicular to the surface to be 1.36 Å long and the other two at 1.26 Å each. The adsorption energy of this configuration is 0.66 eV. On the negative surface the surface termination is again distorted by the formation of Nb−O−Li−O−Nb bridge structures. The CO_2 molecule adsorbs close to one of these bridges, sharing an oxygen atom to form a

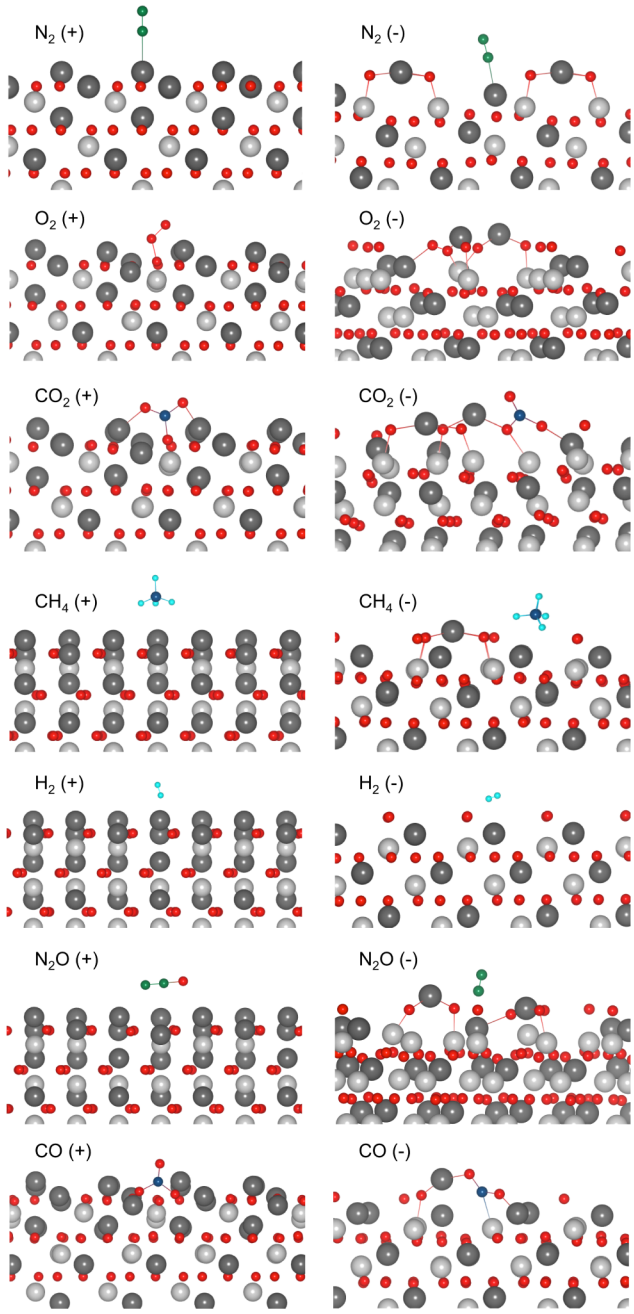

Figure 3. Adsorption geometries of N_2, O_2, CO_2, CH_4, H_2, N_2O, and CO at the positive (left-hand side) and negative (right-hand side) LN(0001) surface. Atomic color coding as in Figure 2

CO_3-like structure. The C−O bond pointing away from the surface is 1.23 Å long, the others are 1.36 and 1.33 Å, respectively. Thus, the C−O bond lengths at the positive and at the negative surface are between 6% and 8% larger than in the free-standing CO_3 molecule. The adsorption energy at the negative side amounts to 1.44 eV. The charge distribution indicates chemisorbed molecules (Figure 4).

CH_4 adsorbs on both surfaces without remarkable distortion (see Figure 3). The molecule adsorbs almost on top of the topmost Li atom, however rather far from the surface, namely 2.5 Å above the positive surface and of 2.2 Å above the negative surface, further than any other investigated molecule. The previously mentioned bridge-like structures are formed at the negative surface. The adsorption energies are limited to 0.08

dx.doi.org/10.1021/jp502936f | J. Phys. Chem. C 2014, 118, 10213−10220

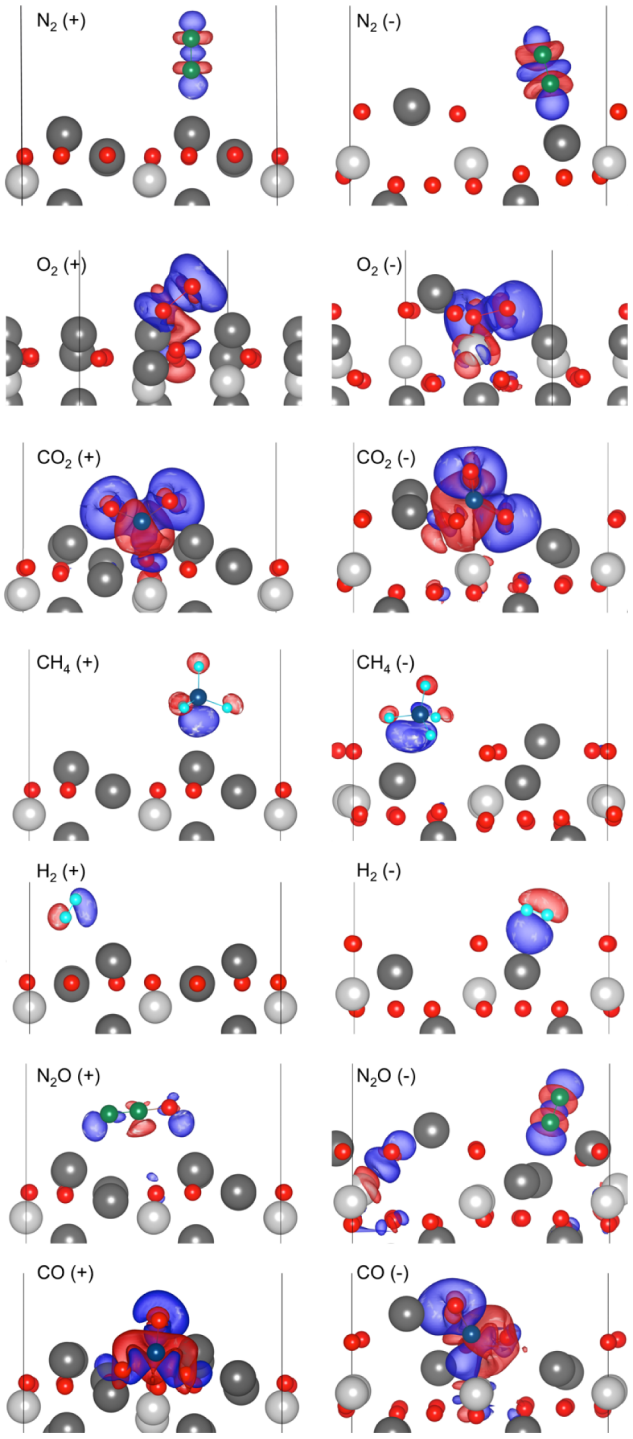

Figure 4. Charge redistribution upon adsorption of N_2, O_2, CO_2, CH_4, H_2, N_2O, and CO at the positive (left-hand side) and negative (right-hand side) LN(0001) surface. Atomic color coding as in Figure 2, red indicates charge depletion and blue indicates charge accumulation.

and 0.31 eV at the $+z$ and $-z$ surface, respectively. Adsorption energy, structural configuration and charge redistribution limited to the molecular neighborhood suggest a physisorption of CH_4 at both LN(0001) surfaces.

Similarly, H_2 shows a rather limited interaction with the surface. On the $+z$ surface the favored adsorption sites are spread over the unit cell with differences only in the meV range. The most favored adsorption site between the oxygen and lithium atoms of the surface leads to an adsorption energy of 0.06 eV. The situation is similar at the $-z$ cut surface, with an adsorption energy of about 0.16 eV. The main difference between the two polarization directions is the orientation of the H_2 dimer, which is perpendicular to the positive and parallel to the negative surface. H_2 is the only molecule that causes no distortion of the $-z$ surface of LN, and can be seen as a prime example of physisorbed molecules.

N_2O (laughing gas) adsorbs lying relatively flat on the $+z$ surface with an adsorption energy of 0.19 eV in a height of about 2 Å above the highest Li atom. Similar to all the other molecules on this surface, it does not noticeably affect the substrate morphology. The molecular geometry itself is as well only slightly distorted. This picture changes remarkably on the negative surface where the adsorption occurs dissociatively. Different combinations of the spontaneously dissociated molecule can be found for different starting configurations. The most favored structure consists of a N_2 molecule lying 2.75 Å above a lithium atom and of an (isolated) oxygen atom integrated in a bridge-like structure (Figure 3). This configuration leads to an adsorption energy of 3.02 eV. Thus, nitrous oxide seems to be physisorbed at the positive LN(0001) and chemisorbed at the negative LN(0001).

CO forms different structures at different LN z surfaces. At the $+z$ surface it forms, similarly to CO_2, a structure reminiscent of the CO_3 configuration. Thereby bond lengths of 1.33 Å for the bonds pointing to the surface and 1.24 Å for the bond pointing out from the surface are calculated. This structure leads to an adsorption energy of 3.84 eV, the highest adsorption energy on this surface among the here considered molecules. At the $-z$ surface the molecule is integrated in a bridge-like structure reminiscent of a bent CO_2 molecule with bond lengths of 1.25 Å (pointing away from the surface) and 1.33 Å (parallel to the surface). The free-standing CO_2 molecule[22] has bond lengths of 1.16 Å and thus is substantially stretched upon adsorption.

One common feature of all the investigated adsorbates is their rather different impact at the two z surfaces. While the $+z$ surface is not distorted upon adsorption (excluding a minor displacement of the oxygen atoms close to the adsorption site), the $-z$ surface morphology is strongly influenced by all investigated adsorbates, excluding H_2 which is almost completely inert. As a common feature, Li atoms are extracted from the $-z$ surface to form bridge structures which increase the surface relaxation and lower the system energy. This is not surprising, as the negative LN(0001) surface is known to be much more reactive than the positive. As an example, the etching rate at the negative surface is orders of magnitude larger than at the positive surface.[26] Thus, the extraction of Li atoms from the $-z$ surface upon molecular adsorption can be interpreted as the onset of etching phenomena. We remark that the calculated adsorption energies model the molecular adsorption of single and isolated adsorbates on an undistorted surface. Adsorption on surfaces distorted by thermal effects or by the presence of other adsorbates or surface defects (e.g., ferroelectric domain boundaries) may result in significantly higher adsorption energies.

The adsorption energy of the investigated molecules is by far lower than the sum of the adsorption energies of the single atoms building the molecule (see Table 1). However, this does not mean that the adsorption of the investigated molecules occurs dissociatively. To realize spontaneous dissociation, the adsorption energy of the molecular components has to be higher than the binding energy of the atoms within the

dx.doi.org/10.1021/jp502936f | J. Phys. Chem. C 2014, 118, 10213−10220

considered molecule, and the atomic adsorption sites have to be within the molecular extension. The first condition is satisfied for the H_2, O_2, CH_4, and the N_2O molecule. However, only the latter satisfies also the second condition. Thus, only for nitrous oxide spontaneous dissociative adsorption is expected, while for the other considered adsorbates the dissociation is less likely.

The work function modification upon molecular adsorption is investigated in order to identify the direction of the charge transfer between molecule and substrate. This also allows a determination of whether the adsorbates contribute to stabilize the surface by charge compensation. The work function modifications upon adsorption are reported in Table 2. The

Table 2. Work Functions Φ of the Clean LN(0001) Surface and Differences ΔΦ upon Molecular Adsorption for the Positive (Left Hand Side) and Negative (Right Hand Side) Surface. All Values Are in Electron Volt

adsorbate	Φ_p	$\Delta\Phi_p$	Φ_n	$\Delta\Phi_n$
none	6.13		4.59	
N_2	6.46	+0.33	3.26	−1.33
O_2	7.17	+1.04	5.19	+0.60
CO_2	7.73	+1.60	3.69	−0.90
CH_4	6.46	+0.33	3.67	−0.92
H_2	6.55	+0.42	5.51	+0.93
N_2O	6.49	+0.36	5.68	+1.09
CO	5.41	−0.73	4.03	−0.56

values of the work functions of 6.13 and 4.59 eV calculated for the clean positive and negative LN(0001) surfaces are in good agreement both with previous calculations[10] and UV-PEEM measurements,[12] estimating the work functions in 6.2 and 4.6 eV for the positive and for the negative surface, respectively. The $+z$ surface is characterized by electronic charge accumulation, while the $-z$ surface is characterized by an electronic charge depletion.[2,6] Thus, molecules acting as electronic charge acceptors might stabilize the positive surface by charge compensation, while adsorbates acting as electron donors may stabilize the negative surface. As a general trend, in the case of physisorbed adsorbates the substrate work function is reduced as a consequence of a molecule-to-substrate electron transfer. Vice versa, an increased work function suggests a substrate-to-molecule electron transfer. This picture does not necessarily hold for chemisorbed systems, as the interface charge rearrangement determined by bond formation might complicate the situation. The outlined trend is clearly mirrored in our calculations. At the positive surface, all the adsorbates induce a work function increase apart from CO which is clearly chemisorbed. This suggests that surface stabilization by charge compensation via adsorbate capture is a major mechanism at the polar LN(0001). Accordingly, all the investigated adsorbates apart from N_2O, O_2, and H_2 lower the work function at the negative side. While the first two are clearly chemisorbed, H_2 can hardly transfer electrons to the surface. Concerning the chemisorbed species, as expected, the strongly electronegative O_2 and N_2O molecules capture electrons from the substrate, irrespective of the surface polarity, while CO acts as a donor both at the positive and at the negative surface.

Desorption Temperature. Equation 1 allows for the calculation of the formation energy of clean and adsorbed surfaces as a function of the chemical potential of the considered molecule, and thus for the determination of the desorption conditions (represented by the chemical potentials). This is defined as the point at which the formation energy of clean surfaces become lower than that of adsorbed surfaces. This is exemplarily shown for the N_2 molecule in Figure 5. It is,

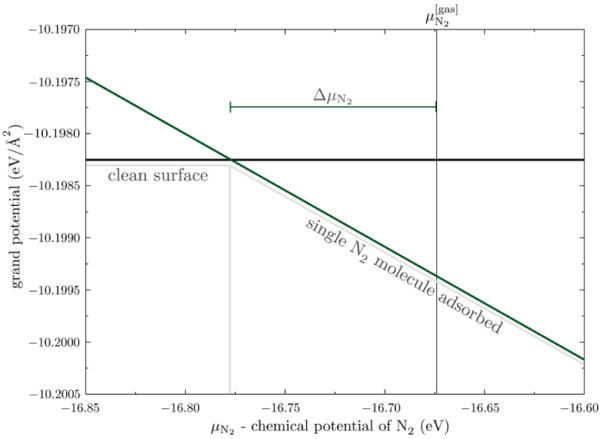

Figure 5. Formation energy of clean and N_2 adsorbed LN(0001) positive surfaces as a function of the N_2 chemical potential. The intersection of the formation energies of the clean and the N_2 adsorbed surface is marked by a vertical gray line, while the value of the chemical potential of the reference phase $\mu_{N_2}^{gas}$ is indicated. The difference of these values is defined as $\Delta\mu_{N_2}$.

however, desirable to have the phase diagrams dependent on directly accessible experimental quantities such as temperature and pressure. Using eq 2 it is possible to express the chemical potential in terms of temperature and molecular partial pressure. To compare the phase diagrams of different molecules, the molecular partial pressure is converted into total pressure. This is done again in the framework of the ideal gas approximation, considering the molecular partial pressure as proportional to the volume percentage in air of the molecule. While the volume percentage of most of the considered adsorbates in air is rather constant, this is not the case for H_2O, whose volume percentage varies extremely. The diagrams for water molecules are calculated using the H_2O volume percentage at room temperature and 50% humidity.

The diagrams in Figure 6 show the conditions at which a given molecule will adsorb/desorb at/from the surface. For a combination of temperature and a pressure above a curve, the molecule would be present at the surface, below it clean surfaces are thermodynamically favored. At ambient conditions, O_2, CO, and H_2O are adsorbed at the LN(0001) positive surface, with desorption temperatures of approximately 1075, 450, and 325 K. These molecules are characterized by the highest adsorption energies, as shown in Table 1. At lower temperatures CO_2 will also be present at the $+z$ surface. The other molecules desorb already at temperatures significantly below 100 K. At the negative surface several molecules adsorb at ambient conditions. O_2 is present under nearly all circumstances (desorption temperature above the ferroelectric phase transition); CO_2, H_2O, and N_2 would desorb at temperatures of 500, 450, and 400 K, respectively. CO desorbs at approximately 260 K, CH_4 at about 120 K, and H_2 at 70 K. Also at the negative surface the desorption temperature order of the different adsorbates mirrors their adsorption energy magnitude. N_2O is not considered at the $-z$ surface as it spontaneously dissociates upon adsorption. It can be observed that in general a given molecule adsorbs at different

dx.doi.org/10.1021/jp502936f | J. Phys. Chem. C 2014, 118, 10213−10220

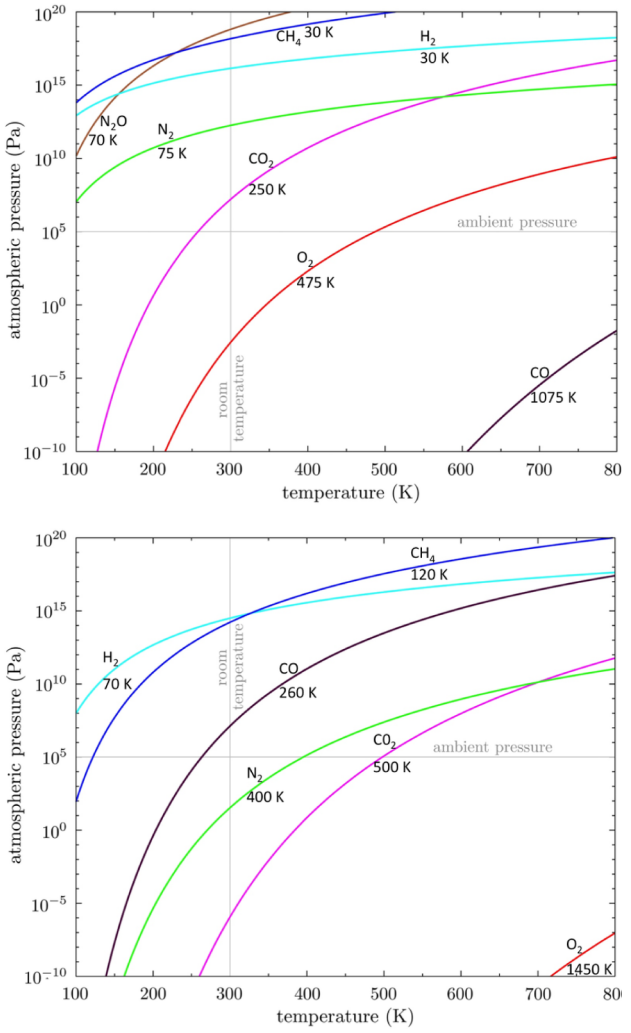

Figure 6. Phase diagrams for the positive (upper part) and negative (lower part) LN surface as a function of temperature and pressure in the presence of the considered adsorbates. The gray lines indicate ambient conditions, for example, room temperature and atmospheric pressure. The temperatures shown below the curves indicate the desorption temperature at atmospheric pressure.

temperatures on differently polarized surfaces. This is in agreement with the X-ray diffraction measurements by Ehre et al.,[27] which first pointed out that water freezes at different temperatures at differently polarized $LiTaO_3(0001)$ surfaces. With the exception of that of CO, the desorption temperatures at the negative surface are higher than at the positive surface.

To take in account the effect of the surface humidity on the desorption temperature, the saturated vapor pressure is calculated via the Magnus equation[28] for the limiting case of 100% humidity. No qualitative differences are observed, and desorption temperature shifts of only a few K are calculated.

CONCLUSION

As a first step toward the understanding of $LiNbO_3$ surfaces at ambient condition, the adsorption of the main air components at the LN(0001) has been simulated. For each of the considered molecules (N_2, O_2, CO_2, CH_4, H_2, N_2O, CO, and H_2O) adsorption sites, energies as well as the interaction with the surface have been determined. The positive surface morphology is found to be relatively unaffected by the adsorbates, while the negative surface undergoes important structural modification upon molecular adsorption. Phase diagrams predicting desorption conditions (temperature and pressure) have been calculated. N_2, CH_4, and H_2 are physisorbed at both the $+z$ and $-z$ LN surfaces and desorb already at low temperatures ($T \leq 120$ K). N_2O is also physisorbed at the $+z$ surface, while it spontaneously dissociates at the $-z$ surface. CO and CO_2 are physisorbed or chemisorbed depending on the surface polarity. O_2 is chemisorbed at both surfaces, instead, and desorbs from the $+z$ surface only for temperatures higher than 475 K. The calculated work function changes allow for the determination of the charge transfer direction upon molecular adsorption. A surface-to-molecule charge transfer is observed for all physisorbed molecules at the positive surface, vice versa a molecule-to-substrate charge transfer characterizes the physisorption at the negative surface. Thus, adsorbate are expected to contribute to the surface stability via charge compensation.

AUTHOR INFORMATION

Corresponding Author

*E-mail: simone.sanna@uni-paderborn.de. Tel.: +49 (0)5251 602333. Fax: +49 (0)5251 603435.

Notes

The authors declare no competing financial interest.

ACKNOWLEDGMENTS

This work has been supported by the DFG (TRR142 and SCHM1361/21). The calculations were done using grants of computer time from the Paderborn Center for Parallel Computing (PC2) and the Höchstleistungs−Rechenzentrum Stuttgart (HLRS).

REFERENCES

(1) Lee, T. C.; Lee, J.-T.; Robert, M. A.; Wang, S.; Rabson, T. A. Surface acoustic wave applications of lithium niobate thin films. *Appl. Phys. Lett.* **2003**, *82* (2), 191−193.

(2) Weis, R. S.; Gaylord, T. K. Lithium Niobate: Summary of physical properties and crystal structure. *Appl. Phys. A* **1985**, *37*, 191−203.

(3) Yun, Y.; Altman, E. I. Using ferroelectric poling to change adsorption on oxide surfaces. *J. Am. Chem. Soc.* **2007**, *129*, 15684−15689.

(4) Wong, K. K. *Properties of Lithium Niobate*; The Institution of Electrical Engineers: London, 2002.

(5) Volk, T.; Wöhlecke, M. *Lithium Niobate: Defects, Photorefraction and Ferroelectric Switching*; Springer: Berlin, 2008.

(6) Sanna, S.; Hölscher, R.; Schmidt, W. G. Temperature dependent $LiNbO_3(0001)$: Surface reconstruction and surface charge. *Appl. Surf. Sci.* **2014**, *301*, 70−78.

(7) Johann, F.; Soergel, E. Quantitative measurement of the surface charge density. *Appl. Phys. Lett.* **2009**, *95*, 232906−232909.

(8) Noguera, C. Polar oxide surfaces. *J. Phys.: Condens. Matter* **2000**, *12*, R367−R410.

(9) Levchenko, S. V.; Rappe, A. M. Influence of ferroelectric polarization on the equilibrium stoichiometry of lithium niobate (0001) surfaces. *Phys. Rev. Lett.* **2008**, *100*, 256101−256105.

(10) Sanna, S.; Schmidt, W. G. Lithium niobate X-cut, Y-cut, and Z-cut surfaces from ab initio theory. *Phys. Rev. B* **2010**, *81*, 214116−214127.

(11) Lushkin, A. Y.; Nazarenko, V. B.; Pilipchak, K. N.; Shnyukov, V. F.; Naumovets, A. G. The impact of annealing and evaporation of $LiNbO_3$ crystals on their surface composition. *J. Phys. D* **1999**, *32*, 22−28.

(12) Yang, W.-C.; Rodriguez, B. J.; Gruverman, A.; Nemanich, R. J. Polarization-dependent electron affinity of $LiNbO_3$ surfaces. *Appl. Phys. Lett.* **2004**, *85*, 2316−318.
(13) Sanna, S.; Rode, S.; Hölscher, R.; Klassen, S.; Marutschke, C.; Kobayashi, K.; Yamada, H.; Schmidt, W. G.; Kühnle, A. Charge compensation by long-period reconstruction in strongly polar lithium niobate surfaces. *Phys. Rev. B* **2013**, *88*, 115422−115427.
(14) Sanna, S.; Hölscher, R.; Schmidt, W. G. Polarization-dependent water adsorption on the $LiNbO_3$ (0001) surface. *Phys. Rev. B* **2012**, *86*, 205407−205415.
(15) Rode, S.; Hölscher, R.; Sanna, S.; Klassen, S.; Kobayashi, K.; Yamada, H.; Schmidt, W. G.; Kühnle, A. Atomic-resolution imaging of the polar $(000\bar{1})$ surface of $LiNbO_3$ in aqueous solution by frequency modulation atomic force microscopy. *Phys. Rev. B* **2012**, *86*, 075468−075472.
(16) Perdew, J. P.; Wang, Y. Accurate and simple density functional for the electronic exchange energy: Generalized gradient approximation. *Phys. Rev. B* **1986**, *33*, 8800−8802.
(17) Kresse, G.; Furthmüller, J. Efficient iterative schemes for *ab initio* total-energy calculations using a plane-wave basis set. *Phys. Rev. B* **1996**, *54*, 11169−11187.
(18) Blöchl, P. E. Projector augmented-wave method. *Phys. Rev. B* **1994**, *50*, 17953−17979.
(19) Neugebauer, J.; Scheffler, M. Adsorbate−substrate and adsorbate−adsorbate interactions of Na and K adlayers on Al(111). *Phys. Rev. B* **1992**, *46*, 16067−16080.
(20) Bengtsson, L. Dipole correction for surface supercell calculations. *Phys. Rev. B* **1999**, *59*, 12301−12304.
(21) Landau, L. D.; Lifshitz, E. M. *Statistical Physics, Part I*; Pergamon Press: Oxford, UK, 1981.
(22) *NIST Standard Reference Database*; http://www.nist.gov/srd/ (accessed November, 2013).
(23) Baghbanpourasl, A.; Hingerl, K.; Wippermann, S.; Schmidt, W. G. Copper(110) surface in thermodynamic equilibrium with water vapor studied from first principles. *Surf. Sci.* **2013**, *612*, 82−89.
(24) Kowalczyk, T.; Krylov, A. I. Electronic structure of carbon trioxide and vibronic interactions involving Jahn-Teller states. *J. Phys. Chem. A* **2007**, *111*, 8271−8276.
(25) Hölscher, R.; Sanna, S.; Schmidt, W. G. Adsorption of OH and H at the $LiNbO_3$ surfaces. *Phys. Status Solidi C* **2012**, *9*, 1361−1365.
(26) Argiolas, N.; Bazzan, M.; Bernadi, A.; Cattaruzza, E.; Mazzoldi, P.; Schiavuta, P.; Sada, C.; Hangen, U. A systematic study of the chemical etching process on periodically poled lithium niobate structures. *Mater. Sci. Eng. B* **2005**, *118*, 150−154.
(27) Ehre, D.; Lavert, E.; Lahav, M.; Lubomirsky, I. Water freezes differently on positively and negatively charged surfaces of pyroelectric materials. *Science* **2010**, *327*, 672−675.
(28) Sonntag, D. Important New Values of the Phys. Constants of 1986, Vapour Pressure Formulations based on ITS-90, and Psychrometer Formulae. *Z. Meteorol.* **1990**, *40*, 340−344.